

# Singular Spectrum Analysis for Tracking of P300

S. Enshaeifar, S. Sanei and C. Cheong Took

**Abstract**—In this work, we introduce a complex-valued singular spectrum analysis for the analysis of electroencephalogram (EEG), which typically exhibits noncircular probability distribution. To exploit such prior knowledge, our technique makes use of recent advances in complex-valued statistics to exploit the power difference or the correlation between the data channels, in contrast to current methods which cater only for the restrictive class of circular data. In particular, the principal component analysis-like technique was employed to detect the onset of P300, and tracked this event-related potential. In this way, the classification of EEG can be made possible to differentiate between a healthy subject and a schizophrenic patient. In particular, we illuminate how features such as P3a and P3b can be used to perform such classification.

## I. INTRODUCTION

**P**RINCIPAL component analysis (PCA) is a well-established statistical algorithm known for its applications in dimensionality reduction, classification and pattern recognition. In 1980s, interests in dynamical systems paved the way for the extension of PCA to singular spectrum analysis (SSA) [1]. Despite being introduced three decades ago in the Statistics community, this technique is relatively unknown to the IEEE Computational Intelligence community, apart from the work in [1].

Singular spectrum analysis (SSA) is a powerful model-free technique which does not need any prior statistical assumption such as normality or Gaussianity of the data [2]. Its application includes single-channel source separation, non-parametric signal decomposition, smoothing and forecasting [2], [3], [4]. SSA has been applied in various areas such as bio-signal processing, image processing, earth science, economics and finance [4], [2], [5]. This work introduces a biomedical application which implements an enhanced version of complex-valued SSA for EEG analysis, particularly for event-related potential (ERP) analysis.

Event-related potentials (ERPs) are specific electroencephalogram (EEG) waveforms in response to different brain stimulations. ERPs have relatively smaller amplitudes compared with the background EEG, thus traditionally ERPs are elucidated using signal-averaging procedure [6]. Analysis of different types of ERPs, such as in visual or auditory stimuli, provides important information for clinical diagnosis of psychiatric diseases such as dementia, alzheimer or schizophrenia [6], [7].

Although ERPs offer fine-grained temporal resolution, they suffer from limited spatial resolution. Furthermore, some of the ERP components are likely to overlap which makes it difficult to distinguish between specific stages of the signal. A common example is the composite P300 wave, which

is a positive ERP component with a latency of about 300 milliseconds after a task-relevant stimuli [6], [7]. P300 is distributed over the midline electrodes (Fz, Cz and Pz) and it generally has larger magnitude towards the parietal electrodes (positioned at the back of the head) [8]. The P300 consists of two major overlapping subcomponents known as P3a and P3b. P3a represents an automatic switch of attention to a novel stimuli regardless of the task, however, P3b is elicited by infrequent task relevant events. P3b wave is mostly central-parietal while P3a has a frontal-central distribution and it is characterized with a shorter latency and more rapid habituation than P3b [6], [9].

Along with other clinical examinations, analysis of P300 could be used as a potential diagnostic procedure. For this purpose, a reliable method for separating P300 subcomponents must be employed. One of the most common methods for P300 detection is the traditional ERP averaging [7]. Averaging over the large number of trials could significantly enhance the P300 wave by reducing the background EEG, however, it suffers from several limitations. For example, averaging assumes that P300 latencies are constant over the time while it is not the case in reality. In addition, this method ignores the effect of brain rapid habituation on P3a [10]. In other words, the person gets used to the stimuli. Thus, it cannot distinguish the small differences between subcomponents which are temporally overlapped [9]. In order to overcome these drawbacks and elucidate the P300 subcomponents, averaging can be applied over the smaller window frames with 50% temporal overlap. This is similar to the concept of single-trial averaging. This method, compared to the overall averaging, would not reduce the background EEG significantly. Therefore, it would be beneficial to apply a robust smoothing algorithm to mitigate the effect of unwanted EEG while extracting the desirable P300 subcomponents.

There are several nonlinear noise reduction algorithms among which singular value decomposition (SVD) based method is widely accepted as an effective method for this purpose [2]. Since SSA is an SVD-based algorithm, it has the potential to be used as a smoothing technique. This work has exploited a novel augmented complex SSA (A-CSSA) rather than traditional SSA to improve the extraction of P300 subcomponents [11]. Complex-valued algorithms can take advantage of the correlation between two similar signals. It is not a surprise, therefore, that they have found many applications in machine learning and EEG analysis. For example, a complex blind source extraction algorithm (C-BSS) was introduced to remove eye artifacts [12].

Moreover, an augmented complex common spatial pattern (AC-CPS) has been developed in [13] for the classification of non-circular EEG during motor imagery tasks. Similarly, this work adapts the recently introduced augmented complex algorithm [11] to detect and track the P300 subcomponents in the classification of healthy and non-healthy subjects.

This paper is organised as follows: a comprehensive overview of the augmented complex SSA algorithm is provided, which is followed by its pseudo-code. We then illustrate how we can make use of this algorithm to enhance the detection of P300 in EEG signals. Finally, the experimental results are provided in section IV and the conclusion in section V.

## II. AUGMENTED COMPLEX SSA ALGORITHM

The objective of SSA is to represent the original signal as sum of a small number of components which can be identified as a trend, periodic or quasi-periodic component or noise<sup>1</sup>. This is achieved by mapping a given signal in terms of eigenvectors and eigenvalues of a matrix generated from the original signal [14]. Fig. 1 illustrates a signal decomposed using basic SSA. It is shown that eigenvalues are placed in decreasing order where top eigenvalues represent the dominant components (Fig. 1,b).

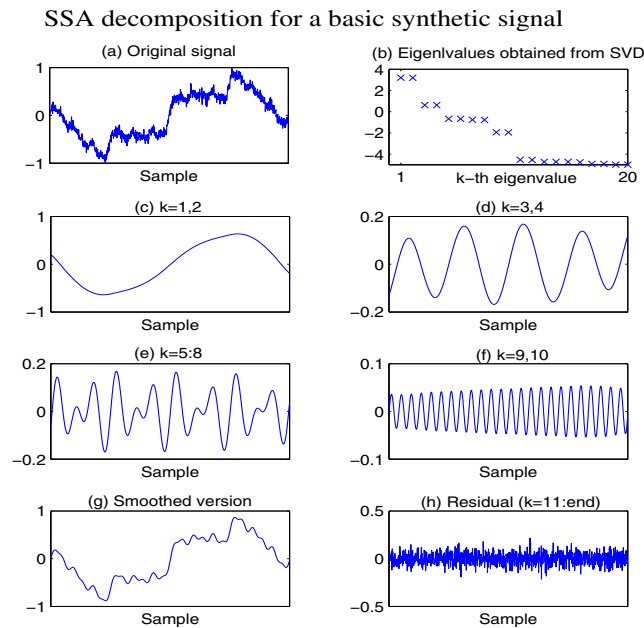


Fig. 1. Simple example for a signal decomposition using basic SSA. According to the eigenvalue subspaces, signal decomposed to the trend (c), periodic and quasi-periodic components (d, e, f) and noise (h). Similar to the concept of PCA, dimensionality is reduced by considering the dominant eigen-subspaces and the smoothed version is shown in (g).

In this work, however, the augmented complex SSA (A-CSSA) was utilised rather than basic SSA. Typically, the statistics of complex domain are considered as the

<sup>1</sup>Observe the similarity to the Empirical Mode Decomposition (EMD), however SSA is a closed form technique, unlike the empirical nature of EMD [14].

direct extension of real domain statistics. For example, the covariance matrix of a zero mean complex vector  $\mathbf{f}$  can be formulated by replacing the standard transpose operator  $(\cdot)^T$  with the Hermitian transpose  $(\cdot)^H$ , i.e.  $\mathbf{f}\mathbf{f}^T \rightarrow \mathbf{f}\mathbf{f}^H$ . However, recent works have shown that basic complex covariance matrix ignores the correlation between the real and imaginary part of the signal; yet this information can be obtained using the pseudo-covariance matrix<sup>2</sup> [15], [16]. Therefore, “augmented” statistics have been established to generalize the optimal second-order statistics for complex domain [15] in which both covariance ( $\mathbf{C}$ ) and pseudo-covariance ( $\mathbf{P}$ ) are considered:

$$\mathbf{f}_a = [\mathbf{f}, \mathbf{f}^*]^T \rightarrow \mathbf{C}_a = E[\mathbf{f}_a \mathbf{f}_a^H] = E \begin{bmatrix} \mathbf{C} & \mathbf{P} \\ \mathbf{P}^* & \mathbf{C}^* \end{bmatrix} \quad (1)$$

To incorporate the latest advances in complex-valued statistics into the CSSA framework, this paper employed the augmented complex SSA (A-CSSA) [11]. SSA algorithm makes use of a special matrix called the trajectory matrix, which can be expressed as follow:

$$\mathbf{W} = \begin{pmatrix} f_1 & f_2 & f_3 & \dots & f_n \\ f_2 & f_3 & f_4 & \dots & f_{n+1} \\ \vdots & \vdots & \ddots & \vdots & \\ f_l & f_{l+1} & f_{l+2} & \dots & f_s \end{pmatrix} \quad (2)$$

The first column in (2) is a segment of the original signal and second column is the one-step lagged version of the first column and so on. All steps of A-CSSA are summarised in Algorithm 1 [14].

---

### Algorithm 1: Augmented complex SSA algorithm

---

#### Decomposition

1. Consider the input as a complex-valued vector  $\mathbf{f}_s$  with length  $s$ .
2. Define the embedding dimension  $l$  as  $1 < l < s$  and  $n = s - l + 1$ .
3. Generate a trajectory matrix  $\mathbf{W}^{l,n}$  using the lagged version of the original signal (Eq. 1).
4. Obtain the augmented version of the trajectory matrix  $\mathbf{W}_a^{2l,n}$  by considering its conjugate (Eq. 2).
5. Calculate the augmented covariance matrix  $\mathbf{W}_a \mathbf{W}_a^H$ .
6. Apply SVD on the generated covariance matrix and produce several eigentriple sets  $(\lambda_j, \mathbf{q}_j, \mathbf{v}_j)^3$ .

#### Reconstruction

7. Select the appropriate subgroups of the eigentriples based on the desirable output.
  8. Generate the new trajectory matrix  $\tilde{\mathbf{W}}_a$  using only selected eigentriples.
  9. Reconstruct the desired complex-valued signal  $\tilde{\mathbf{f}}$  by Hankelization algorithm<sup>4</sup>.
- 

<sup>2</sup>To illustrate the correlation, consider a complex variable  $z = a + jb$ . Its covariance ( $c$ ) can be calculated as  $c = E[zz^*] = E[a^2 + b^2]$  and its pseudo-covariance ( $p$ ) can be defined as  $p = E[zz] = E[a^2 - b^2 + j2ab]$ . The correlation is captured by the term  $E = [j2ab]$

### III. PROPOSED METHOD

Overall averaging can significantly enhance the P300 wave by reducing the background EEG. However, since it is overall average, this method cannot track the temporal changes and distinguish the small differences between subcomponents which are temporally overlapped, such as P3a and P3b. On the other hand, single-trials could track these temporal changes, but they suffer from high EEG background.

Therefore, our proposed method aimed to merge the concept of overall averaging with single-trial analysis. For this purpose, the temporal single-trials were used in parallel with the overall averaged signal known as the reference signal. Thus, each subject has its specific reference ( $\mathbf{x}$ ) calculated from the overall averaging of all the target events. This signal is then combined with a single-trial ERP ( $\mathbf{y}$ ) to construct a one-dimensional complex-valued vector ( $\mathbf{f}$ ) that is,  $\mathbf{f} = \mathbf{x} + j\mathbf{y}$ . Then, the generated complex-valued vector  $\mathbf{f}$  needs to be filtered using the proposed A-CSSA method. As augmented statistics takes into account the correlation between the real and imaginary parts of a signal, the reference signal from the real part of  $\mathbf{f}$  emphasizes the temporal location of P300 in single-trial ERPs by empowering the corresponding eigentriples. Furthermore, as single-trials are measured for short time intervals, it is likely to detect and track the overlapping P300 subcomponents more accurately.

### IV. EXPERIMENTAL RESULT

The proposed method was applied to 12 EEG recorded for 8 healthy subjects and 4 schizophrenic patients during an auditory two-stimuli oddball experiment<sup>5</sup>. In the traditional oddball paradigm an infrequent target randomly occurs in a background of frequent standard stimuli and the subject is told to press a button when the target appears [8], [17].

All experiments were performed on channel Cz. Three main reasons for selecting Cz are: (i) Cz is central channel, so it contains the effect of both P3a and P3b which are distributed frontocentral and centroparietal respectively, (ii) as Cz is found on the central line, it can reflect P300 wave even for abnormal cases with uni-lateral brain difficulties and (iii) posterior alpha wave (8-13Hz) has slightly less effect on the central channel Cz.

The reference signal was obtained by temporally averaging over 35 target events which randomly appeared over a period of 320 seconds. On the other hand, single-trials were calculated over the moving window of 8 target stimuli with 50% temporal overlap. All stimuli, including standards and targets, occurred every 2 seconds. However, in order to increase the chance of P3a generation for the first target, standard stimuli were repeated consecutively for about 50

<sup>3</sup>SVD of the  $\mathbf{W}_a \mathbf{W}_a^H$  produces the corresponding eigenvalues ( $\lambda$ ) and eigenvectors ( $\mathbf{v}$ ,  $\mathbf{q}$ ) of the  $\mathbf{W}_a$ . Thus,  $\mathbf{W}_a$  can be rewritten as the sum of its eigentriples  $\mathbf{W}_a = \sum_j \sqrt{\lambda_j} \mathbf{q}_j \mathbf{v}_j^H$  [14].

<sup>4</sup>Hankelization refers to averaging cross-diagonals elements of matrix ( $\tilde{\mathbf{W}}_g$ ), i.e. averaging along elements with indices ( $i + j = \text{const}$ ).

<sup>5</sup>Data were previously recorded and used in [7]. EEG was originally recorded with a sampling frequency of 2000Hz and it was downsampled to 200Hz for simulation purposes.

seconds and the first target appeared there after to switch the subjects' attention. For more details, see Fig. 2.

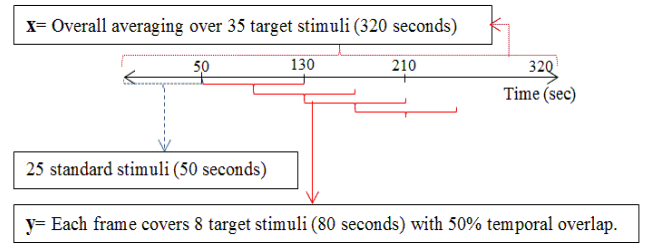


Fig. 2. Each frame has an individual complex-valued signal generated as  $\mathbf{f} = \mathbf{x} + j\mathbf{y}$ . Note that overall average ( $\mathbf{y}$ ) is the same for all frames.

The first frame (50-130sec) for a schizophrenic patient is illustrated in Fig. 3. The frame covers 80 seconds after the first target stimuli. As shown in Fig. 3, P3a and P3b are clearly visible using the proposed A-CSSA method (bottom-right) and their shape was in agreement with the literature [6]. Similar results were observed for 10 subjects.

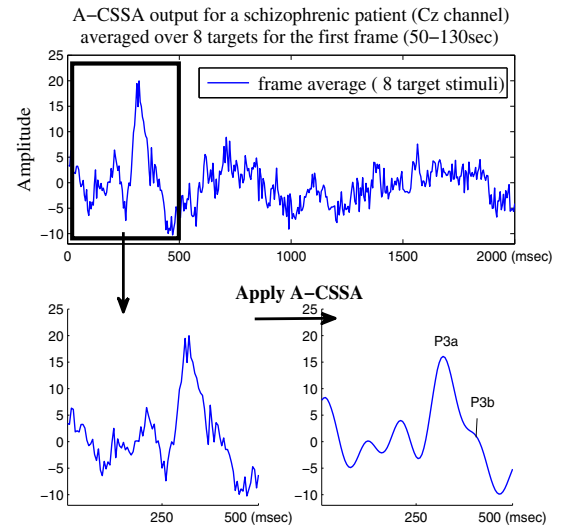


Fig. 3. Original data for a schizophrenic patient recorded from central electrode Cz (top). Original data zoomed in for 1-500msec after the target (bottom left). P300 subcomponents were clearly visible after using A-CSSA (bottom right).

Although P300 subcomponents have the predefined duration ranges, there is no specific narrow-band frequency range to separate them from the strong alpha wave. One of the main advantages of the proposed method, compared to the traditional filtering algorithms, is that A-CSSA does not depend on frequency. Thus, it does not require any prior knowledge of frequency range and it can be applied for either patients or healthy subjects regardless of their P300 features. In order to track the changes in P300 subcomponents, Figure 4 illustrates 250 seconds after the first target for a schizophrenic patient (top middle) and a healthy subject (bottom). Each row in Figure 4 contains four subplots that represent different time frames. According to prior knowledge, P300 is expected within first 500 milliseconds after the

target onset. Hence, all the subplots are zoomed in for this range [7], [8]. Each subplot includes a complex-valued signal in which the real part (dashed line) was a reference signal obtained by averaging of all target stimuli and the imaginary part (solid line) was the average of 8 targets covering the period of 80 seconds. Note that each subject<sup>6</sup> had a unique constant reference for all subplots, see Figure 4.

**Remark#1:** Fig. 4 illustrates the rapid habituation of P3a over time after the first target event. This is the reason why the overall average has less P3a amplitude than frame averaged signal, see Fig. 4 (b and c).

**Remark#2:** As the patient gets used to the stimulus (habituation), which is exhibited by the manifestation of P3a, the P3b visibility improves. Generally, healthy subjects showed faster habituation than schizophrenic patients. Illustratively this is clear from Fig. 4 (c) where P3b is stronger than P3a in the last temporal frame.

**Remark#3:** According to [18], significant reduction of P300 particularly in auditory experiments, is one of the most consistent biological findings in schizophrenia. This work was also in agreement with the literature and it is shown that P3b has constantly lower magnitude in schizophrenic patients (compare Row b and c).

**Remark#4:** In addition to the amplitude differences, schizophrenic patients showed longer P300 latency than healthy subjects (compare Row b and c).

Similar results were observed for 10 subjects, however these are not included due to space limitation. Comparisons were performed by manual observation. However, in future works, we aim to automate the classification process by defining a specific threshold constraints on amplitude and latency of P300 subcomponents.

## V. CONCLUSIONS

In this work, we have shown how biologically meaningful features can be extracted from EEG signal for the classification of healthy subjects and schizophrenic patients. In particular, we have exploited prior knowledge such as known latency of 300 milliseconds to extract these features and made use of recent advances in complex statistics to do so. Moreover, we have introduced the augmented complex-valued singular spectrum analysis (A-CSSA) to combine the traditional averaging method with single-trial ERP analysis in order to attenuate EEG background from the event-related potential P300 so that its tracking can be made possible. Experimental results support our proposed method and are in agreement with the literature.

Future work goes on to (i) develop an automatic detection of P300 subcomponents by defining some constraints based on prior knowledge, (ii) find the optimal window length  $l$  based on the individual datasets and (iii) implement the proposed approach on larger number of data and provide a quantitative evaluation.

<sup>6</sup>These subjects were of the same sex.

## Tracking the P300 subcomponents for a schizophrenic patient vs. a healthy subject

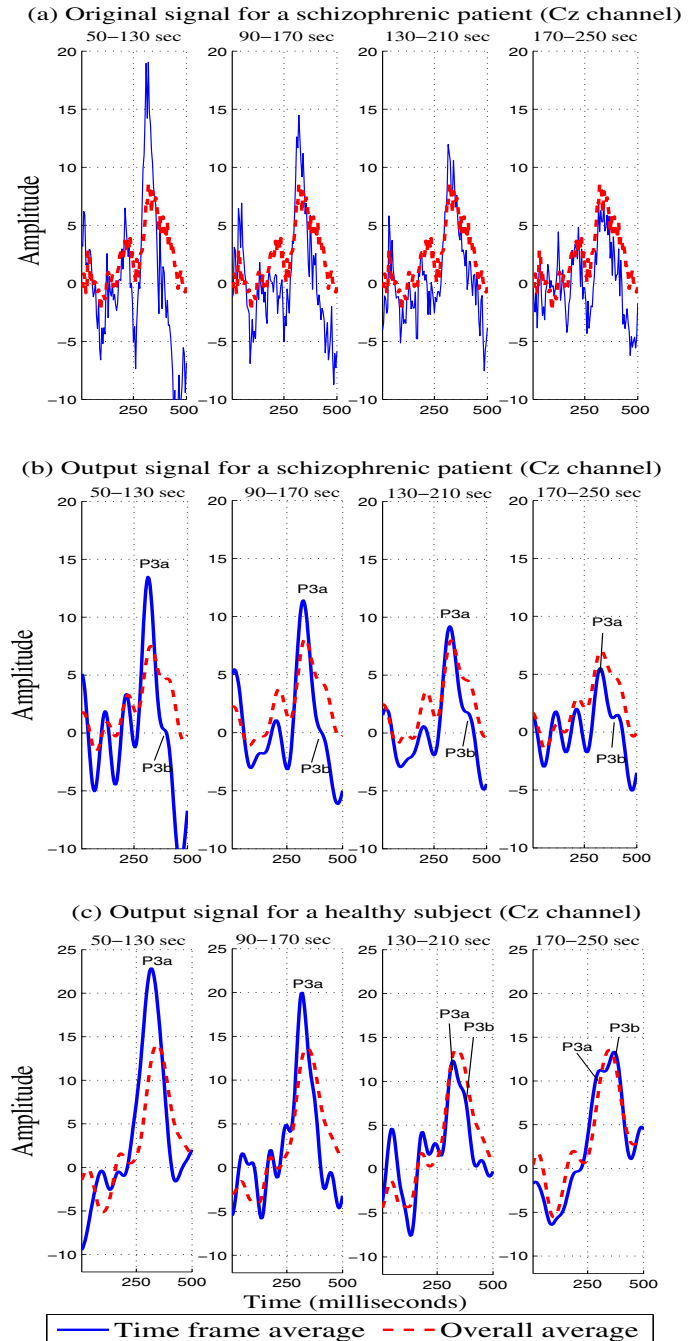


Fig. 4. Original data for a schizophrenic patient (top). Highlighted P300 subcomponents after A-CSSA for the same patient (middle) and a healthy subject (bottom).

## REFERENCES

- [1] W. W. Hsieh and A. Wu, "Nonlinear singular spectrum analysis," in *Proceedings of IEEE International Joint Conference on Neural Networks*, vol. 3, 2002.
- [2] H. Hassani and A. Zhigljavsky, "Singular spectrum analysis: methodology and application to economics data," *Journal of Systems Science and Complexity*, vol. 22, no. 3, 2009.
- [3] S. Sanei, T. K. M. Lee, and V. Abolghasemi, "A new adaptive line

- enhancer based on singular spectrum analysis," *IEEE Transactions on Biomedical Engineering*, vol. 59, no. 2, pp. 428–434, 2012.
- [4] N. Golyandina, V. Nekrutkin, and A. Zhigljavsky, *Analysis of time series structure: SSA and related techniques*. Boca Raton, Florida: Chapman and Hall, 2001.
- [5] S. Sanei and H. Hassani, *Singular Spectrum Analysis of Biomedical Signals*. Taylor & Francis Group-CRC Press, 2014.
- [6] S. Sanei, *Adaptive processing of brain signals*. John Wiley & Sons, 2013.
- [7] L. Spyrou, M. Jing, S. Sanei, and A. Sumich, "Separation and localisation of P300 sources and their subcomponents using constrained blind source separation," *EURASIP Journal on Applied Signal Processing*, vol. 2007, no. 1, pp. 89–89, 2007.
- [8] J. Polich, "Updating P300: an integrative theory of P3a and P3b," *Clinical neurophysiology*, vol. 118, no. 10, pp. 2128–2148, 2007.
- [9] L. Spyrou and S. Sanei, "A robust constrained method for the extraction of P300 subcomponents," in *Proceedings of IEEE International Conference on Acoustics, Speech and Signal Processing, 2006*.
- [10] J. M. Ford, "Schizophrenia: the broken P300 and beyond," *Psychophysiology*, vol. 36, no. 6, pp. 667–682, 1999.
- [11] S. Enshaeifar, S. Sanei, and C. C. Took, "An eigen-based approach for complex-valued forecasting," *ICASSP 2014*.
- [12] S. Javidi, D. P. Mandic, C. C. Took, and A. Cichocki, "Kurtosis-based blind source extraction of complex non-circular signals with application in eeg artifact removal in real-time," *Frontiers in neuroscience*, vol. 5, 2011.
- [13] C. Park, C. Cheong Took, and D. Mandic, "Augmented complex common spatial patterns for classification of noncircular eeg from motor imagery tasks," *IEEE Transactions on Neural System and Rehabilitation engineering*, vol. 22, no. 1, pp. 1–10, 2014.
- [14] N. Golyandina and A. Zhigljavsky, *Singular spectrum analysis for time series*. Springer, 2013.
- [15] D. P. Mandic and S. L. Goh, *Complex valued nonlinear adaptive filters: noncircularity, widely linear and neural models*. Wiley, 2009.
- [16] P. J. Schreier and L. L. Scharf, *Statistical Signal Processing of Complex-Valued Data*. Cambridge University Press, 2010.
- [17] J. Polich and J. R. Criado, "Neuropsychology and neuropharmacology of P3a and P3b," *International Journal of Psychophysiology*, vol. 60, no. 2, pp. 172–185, 2006.
- [18] E.-J. Park, S.-I. Han, and Y.-W. Jeon, "Auditory and visual P300 reflecting cognitive improvement in patients with schizophrenia with quetiapine: A pilot study," *Progress in Neuro-Psychopharmacology and Biological Psychiatry*, vol. 34, no. 4, pp. 674–680, 2010.